Proceedings Paper:
Doychinov, V orcid.org/0000-0001-6730-0057 and Robertson, ID (2022) Radio Wave Propagation Inside Buried Sewer Pipes for Infrastructure Robotics. In: 2021 51st European Microwave Conference (EuMC). 2021 51st European Microwave Conference (EuMC), 04-06 Apr 2022, London, UK. IEEE , pp. 982-985. ISBN 978-2-87487-063-7

https://doi.org/10.23919/EuMC50147.2022.9784221

Radio Wave Propagation Inside Buried Sewer Pipes for Infrastructure Robotics

Viktor Doychinov[#1], Ian D. Robertson[#]

[#]Institute of Robotics, Autonomous Systems, and Sensing, School of Electronic and Electrical Engineering,
University of Leeds, UK
[1]v.o.doychinov@leeds.ac.uk

***Abstract*— Infrastructure robotics hold the potential to improve the maintenance of buried infrastructure, thus saving time, money, and effort. Here we present theoretical and experimental investigation of radio wave propagation inside buried sewer pipes, for the purposes of enabling the command and control of such robots. Good agreement between modelled and measured results lay the foundations for the development of system-level models for underground wireless networks.**

***Keywords*— propagation, lossy waveguide, communication, robotics**

I. Introduction

The reactive maintenance of buried infrastructure, such as potable water and sewer pipes, can be a major source of expenditure for utilities companies, and an inconvenience to end-users [1]. Autonomous robots, that can be inserted into these pipes, and traverse them regularly to inspect their condition and detect any leakages and blockages, have been identified as a way to switch from reactive to proactive maintenance and as a result save money, downtime, and improve the end-user experience [2].

Such robots will necessarily need to have a wireless communication link to a monitoring station established at all times, for the purposes of command and control, retrieval, and timely updates [3]. Currently, there are few studies who have examined this issue. The ones that exist focus either on direct pipe-to-ground communication [4], or investigate the problem empirically in a limited set of circumstances [5], [6].

In this contribution, we present the first step towards enabling such links through the theoretical analysis and field measurements of radio wave propagation inside buried sewer pipes. A key novelty is the modelling approach, aimed at deriving a generally applicable methodology, and providing an explanation of the measured results through fundamental electromagnetic propagation theory.

II. Analytical & Numerical Modelling

From an electromagnetic point of view, empty sewer pipes buried in soil are similar to tunnels, mine shafts, and underground railways. They can all be modelled as hollow waveguides in a lossy dielectric medium, with a different cross-section, circular in the case of sewer pipes.

The theoretical analysis of electromagnetic propagation inside such waveguides is well developed, with multiple experiments confirming the analytical results [7]. Generally, finding the propagation constants γ_{nm} of the various modes in such a waveguide involves solving a transcendental equation. However, this can be greatly simplified if the waveguide is electrically large compared to the wavelength of interest, i.e [8].

$$\pi a/\lambda \gg |\nu|\, u_{nm} \tag{1}$$

Where a is the diameter of the circular cross-section of the waveguide, λ is the free-space wavelength, u_{nm} is the solution to $J_{n-1}(u_{nm}) = 0$, and ν is the square root of the complex relative permittivity of the surrounding medium.

It should be noted that while (1) is generally fulfilled for road tunnels with widths and heights of several metres and mobile phone frequencies, that is not the case for sewer pipes, which most often have diameters of 300 mm or less [9], and the sub-6 GHz licence-exempt frequencies. Nevertheless, the approximate solutions are a good starting point due to their computational efficiency.

Key lessons learned from the work on propagation inside lossy waveguides, which are applied to this work on sewer pipes, are that higher frequencies suffer less loss per unit length [7], and that there are several zones along the axial distance of the waveguide where different modes of propagation take place [10].

The first one is free-space, which occurs at distances such that the first Fresnel zone is fully contained within the diameter of the waveguide. This is followed by a multi-mode zone, where waveguide mode propagation begins. Finally, as the higher-order modes attenuate, there is a transition to single-mode propagation. Generally speaking, the types of modes that can propagate inside circular lossy waveguides are EH_{nm}/HE_{nm}, TE_{0m}, and TM_{0m} [7].

Therefore, the overall propagation loss L_{tot} for a given distance d_{tot} can be expressed as [7]:

$$L_{tot} = 20\lg\sum_{i=1}^{N}\left|e^{-\gamma_i(d_{tot}-d_{fs})}\right| + L_{fs}(f, d_{fs}) \tag{2}$$

Where γ_i are the complex propagation constants for the first N modes taken into consideration, expressed as $\alpha + j\beta$ with α in Np/m and β in rad/m; d_{fs} is the maximum free-space distance calculated using the formula for the first Fresnel zone [11]; and L_{fs} is the free-space propagation loss at that distance, calculated using the well-known Friis formula [11].

As will be shown in Section III, the intention is to apply this model to a 225 mm diameter concrete pipe buried in dry sand and compare the results to field measurements. The frequencies of interest are 2450 MHz and 5800 MHz, the two highest sub-6 GHz licence-exempt frequencies. The d_{fs} for these two frequencies was calculated as 0.38 m and 0.97 m, respectively. Since it was impractical to measure the complex relative permittivity of the sand at the time, the model described in [12] was used to obtain a value of $2.5331 - j0.0303$ for 2450 MHz and $2.5306 - j0.0141$ for 5800 MHz. Substituting all these values in the approximate expression for γ_{nm} in [8] for the first 10 modes yields the propagation constants summarised in Table 1. It can be seen clearly that this particular pipe in this particular environment is incredibly lossy, particularly at 2450 MHz.

The final step in this preliminary analysis was to run EM simulations of the experimental setup in order to qualitatively confirm the expected behaviour. The Finite-Difference Time-Domain (FDTD) simulator gprMax was used for this purpose, as it is well suited for investigating electromagnetic wave interaction with soils [13].

Plots of the magnitude of the Poynting vector $\boldsymbol{S}$ in dB at 2450 MHz and 5800 MHz are shown in Fig. 1 and Fig. 2, respectively. The simulation results confirm our expected behaviour, with free-space, multi-mode, and single-mode regions clearly present. However, in the case of 5800 MHz, the simulation shows that the break point between the free-space and waveguide modes occurs at a smaller distance, or 0.273 m in this case. This was the value used in Section III when calculating the overall expected propagation loss.

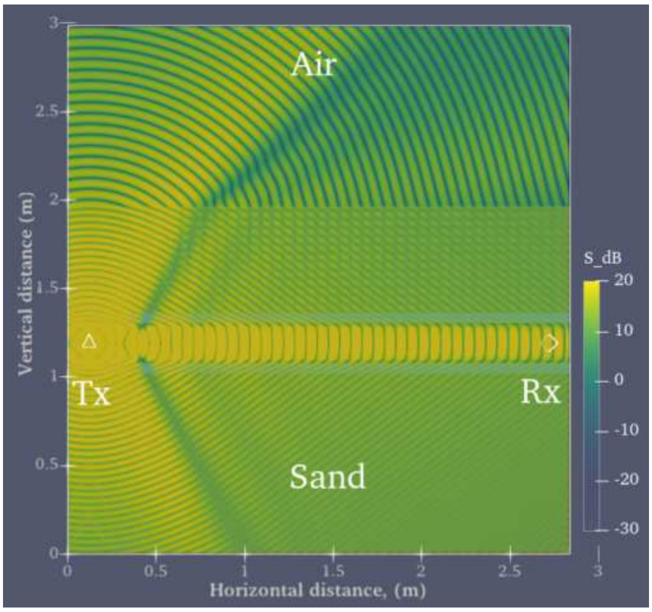

Fig. 1. Snapshot of a CW propagating at 2450 MHz. Shown is the vertical cross-section through the centre of the pipe.

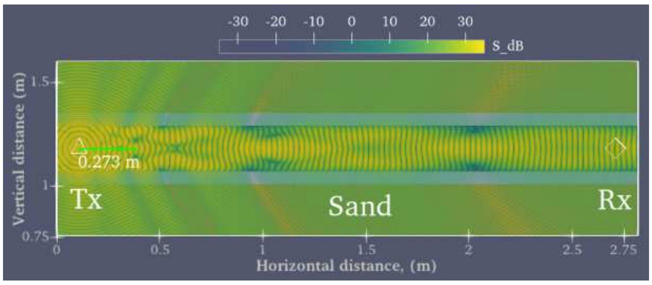

Fig. 2. Snapshot of a CW propagating at 5800 MHz. Shown is the vertical cross-section through the centre of the pipe. Included is the measured distance to the break point between free-space and waveguide mode propagation. Due to memory limitations only part of the setup is shown.

III. Experimental Setup & Measurement Results

A. *Sewer Pipe*

All experiments and measurements reported here took place at the National Laboratory for Distributed Water Infrastructure, part of the the Integrated Civil and Infrastructure Research Centre (ICAIR) at the University of Sheffield in the UK. The Laboratory houses a test cell with an empty sewer pipe, buried in homogeneous, dry sand. While the facility has the capability to provide water flow at various velocities and levels, those were not used during these initial experiments.

Table 1. Propagation constants for the first 10 modes in the sewer pipe under investigation. Values given for the two frequencies of interest.

Mode	2450 MHz		5800 MHz	
	α, [dB/m]	β, [rad/m]	α, [dB/m]	β, [rad/m]
EH_{11}	19.07	46.8943	3.41	119.6790
TE_{01}	27.23	40.0210	4.96	116.7848
HE_{21}	48.41	40.0449	8.66	116.7868
TM_{01}	69.60	40.0689	12.37	116.7888
HE_{31}	86.97	31.0431	15.66	112.9863
TE_{02}	91.29	13.7360	16.62	105.5545
HE_{12}	100.48	27.8892	17.98	111.6547
TE_{03}	191.97	-28.5020	34.94	87.9038
HE_{13}	246.94	-6.3053	44.18	97.2179
HE_{23}	341.29	-28.3333	61.07	87.9178

The section of the buried sewer pipe which was used is described in more detail in Fig. 3. The pipe itself is approximately 3.3 metres long, made of concrete, with a diameter of 225 mm and buried in approximately 0.8 metres of sand. Access to the pipe is through two manholes. The condition of the pipe is near-pristine, with only small traces of residue along its bottom.

This combination of factors makes this test bed ideal for baseline, best-case scenario measurements, since all variables influencing the propagation behaviour are known. However, it is important to note that sewer pipes in active use will present a much more challenging electromagnetic environment due to the overall condition of the pipes, the presence of sewerage and water flow, as well as the wide variety of surrounding soils and burial depths.

B. *Test & Measurement Equipment*

Due to the size and nature of the pipe being measured, the authors could not use standard benchtop microwave test and measurement equipment. Instead, a combination of Software

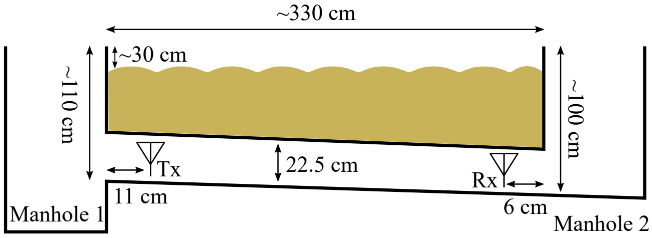

(a) Vertical cross-section drawing

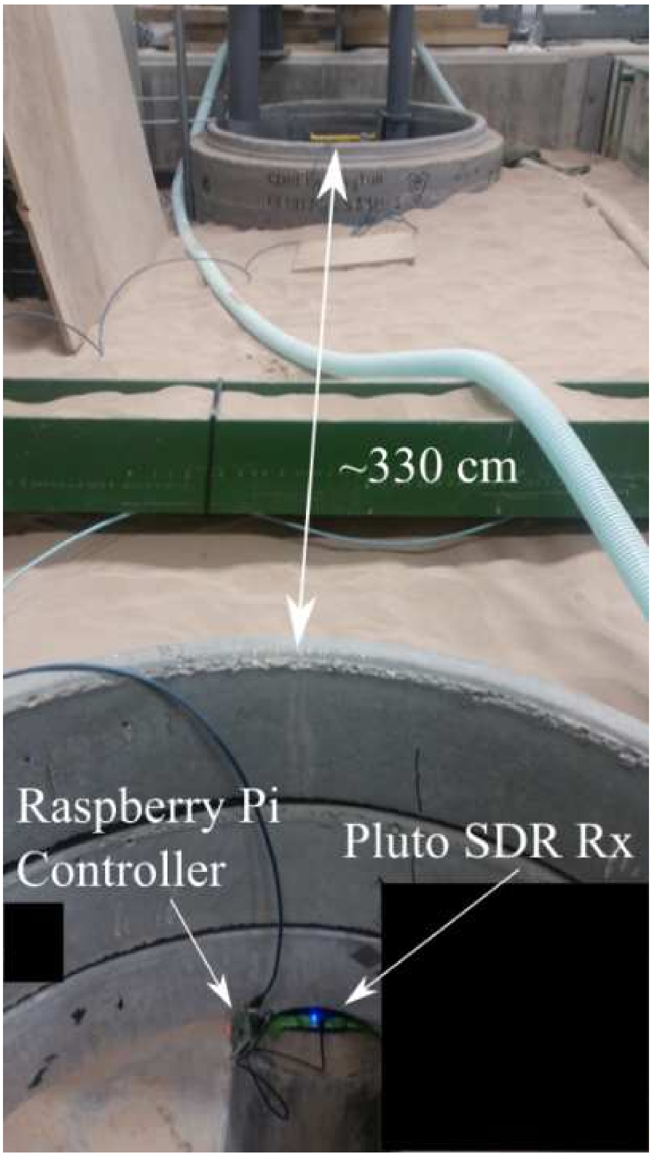

(b) Above ground photograph. Co-located equipment of commercially sensitive nature has been blocked with black rectangles.

Fig. 3. Pipe section used for experiments at ICAIR's sandpit, including key dimensions and distances.

Defined Radio (SDR) modules and Single Board Computers (SBC) was used to provide a signal generator and a signal analyser functionality.

In particular, two Analog Devices Pluto SDR modules were used, each controlled by a Raspberry Pi, which in turn were powered through a Power over Ethernet (PoE) switch. The SDR units themselves were positioned roughly in the middle of the pipe cross-section using 3D printed holders. Finally, commercially available dipole antennas were used to send and receive the signals.

(a) Vertical orientation (b) Horizontal orientation

Fig. 4. Two different orientations used for the transmitter and receiver dipole antennas. Also pictured a Pluto SDR unit in its holder.

A preliminary calibration step was performed in laboratory conditions, to measure the absolute output power of the SDR units at different frequencies in dBm, as well as to relate the readings of their Analog-to-Digital Converters (ADCs) in dBFS to absolute values in dBm. The instruments used for the calibration were a Keysight N9030A Signal Analyser and a Keysight E4438C Signal Generator. Care was taken to ensure that the same configuration of the SDR units was maintained between the calibration measurements and the field experiments. In particular, the hardware gain mode of the receiver was switched to "manual" and maintained at 20 dB.

Both horizontal and vertical antenna orientations, as illustrated in Fig. 4, were used. Due to the relative positioning of the antenna to the pipe cross-section, it is expected that all possible modes, i.e. EH_{nm}/HE_{nm}, TE_{0m}, and TM_{0m} will be excited.

While the position of the receiver unit was maintained constant, at an offset of 6 cm from the pipe end, measurements were taken for two positions of the transmitter unit, at an offset of 11 cm and 56 cm. The overall antenna-to-antenna separations, taking into account the offsets from the pipe ends and the length of the SDR units, were 2.83 metres and 2.38 metres, for the two transmitter positions respectively.

C. Measurement Data

Measurements were taken on multiple days at two different ISM frequencies, 2450 MHz and 5800 MHz, under Continuous Wave (CW) excitation. Data was recorded as time domain samples, with each measurement consisting of 32768 samples at 1.024 Msps, capturing 32 ms of signal. Each such measurement was then converted to the frequency domain using the Fast Fourier Transform, and the received power of the CW tone recorded.

This was repeated for different antenna orientations and for the two transmitter positions. For each of these, 300 measurements were taken and subsequently averaged. Overall, there was little variation between different orientation, e.g. at 5800 MHz with both antennas horizontal the propagation loss was on average 42 dB, whereas with both antennas vertical the loss was on average 45 dB.

Table 2. Comparison between measured and calculated loss inside the sewer pipe for the two different link distances.

Frequency	**Measured,** $d = 2.83m$	**Calculated**	**Difference**
2450 MHz	73.7 dB	78.9 dB	5.2 dB
5800 MHz	42.4 dB	41 dB	-1.4 dB
Frequency	**Measured,** $d = 2.38m$	**Calculated**	**Difference**
2450 MHz	60.9 dB	69.4 dB	8.5 dB
5800 MHz	34.7 dB	37.3 dB	2.6 dB

D. *Results and Discussion*

Once the experimental propagation losses at 2450 MHz and 5800 MHz were obtained, they were subsequently compared to those predicted using the analytical models described in Section II. For the purposes of (2), the propagation constants of the first three modes from Table 1 were used for 2450 MHz, whereas all but HE_{23} were used for 5800 MHz.

The results are summarised in Table 2, where the difference is calculated as $L_{calc} - L_{meas}$.

The comparison can be interpreted to show that the electrically-large approximation can be used to successfully model the propagation loss in sewer pipes even for frequencies for which the approximation condition (1) is not satisfied. It is also clear that accuracy improves as the frequency increases.

However, these results would not have been as accurate if gprMax had not been used to estimate the position of the break point between the free-space mode and the waveguide mode at 5800 MHz. Further experiments and simulations are necessary to investigate in what cases this break point occurs at shorter distances than expected.

Other factors that can explain the differences between the measured and predicted losses include the absence of the concrete pipe shell in the analytical model, the gain and coupling loss of the individual antennas, the effect of the surface roughness of the inside pipe surface, as well as overall variance in the complex relative permittivity of the sand, inaccuracies in distance measurements, and hardware performance variability.

It should be noted that despite all these factors, the differences are not that significant from a practical point of view. Taking the attenuation constant of the lowest-loss mode, EH_{11} as a lower bound for the loss in the single-mode region, the difference of 8.5 dB in the case of 2450 MHz corresponds to a distance of 0.45 metres; whereas the difference of 2.6 dB in the case of 5800 MHz corresponds to a distance of 0.76 metres.

In any case, these results pose interesting challenges for the design and development of a sewer pipe wireless communications network. Given that access points into the sewerage network are spaced at least 100 metres apart, providing continuous coverage for autonomous robots would almost certainly require relay stations and convoy mesh networking.

IV. Conclusion & Future Work

We have presented the applicability of the established lossy waveguide propagation theory to the case of buried, empty sewer pipes. This is a first step towards building a framework for the system-level design of a wireless communications network that can support autonomous robots continuously inspecting said pipes.

As expected, higher frequencies experience less loss and as a result will propagate farther inside buried pipes. This makes the option of using millimetre-wave communication at 60 GHz attractive, as that can also support much higher data rates.

Further work will focus on exploring these and other concepts such as in-pipe linear mesh networks, as well as refining the theoretical framework against measurements in different environments. Of particular interest will be investigating how pipe fill level will affect the propagation and what the best ways to model that can be.

Acknowledgement

This work is supported by the UK's Engineering and Physical Sciences Research Council (EPSRC) Programme Grant EP/S016813/1.

The authors are thankful to Dr Will Shepherd and Dr Christopher Parrott, for their help with setting up the measurements in the sewer pipe.

References

[1] L. O. Makana, N. Metje, I. Jefferson, M. Sackey, and C. D. F. Rogers, "Cost estimation of utility strikes: towards proactive management of street works," *Infrastructure Asset Management*, vol. 7, 2018.

[2] C. Rogers, D. Chapman, N. Metje, and M. E. Torbaghan, "Assessing the Underworld - a Three-Infrastructure Approach to Remote Sensing," Florence, Italy, 2019.

[3] H. Ogai and B. Bhattacharya, *Pipe Inspection Robots for Structural Health and Condition Monitoring*. New Delhi: Springer India, 2018, vol. 89.

[4] S. Mekid, D. Wu, R. Hussain, and K. Youcef-Toumi, "Channel modeling and testing of wireless transmission for underground in-pipe leak and material loss detection," *International Journal of Distributed Sensor Networks*, 2017.

[5] W. You, D. Wu, H. Ogai, K. Hirai, T. Abe, and G. Sato, "Wireless radio communication system for a pipe inspection robot," in *Proceedings of the 13th International Symposium on Artificial Life and Robotics, AROB 13th'08*. IEEE, 2008.

[6] T. Nagashima, Y. Tanaka, and S. Ishihara, "Measurement of wireless communication characteristics in sewer pipes for sewer inspection systems using multiple wireless sensor nodes," in *2015 IEEE 26th Annual International Symposium on Personal, Indoor, and Mobile Radio Communications (PIMRC)*. IEEE, 2015.

[7] D. G. Dudley, M. Lienard, S. F. Mahmoud, and P. Degauque, "Wireless propagation in tunnels," *IEEE Antennas and Propagation Magazine*, 2007.

[8] E. A. J. Marcatili and R. A. Schmeltzer, "Hollow metallic and dielectric waveguides for long distance optical transmission and lasers," *The Bell System Technical Journal*, 1964.

[9] D. Butler, C. Digman, C. Makropoulos, and J. W. Davies, *Urban Drainage*. CRC Press, 2018.

[10] K. Guan, Z. Zhong, B. Ai, R. He, B. Chen, Y. Li, and C. Briso-Rodríguez, "Complete Propagation Model in Tunnels," 2013.

[11] S. Salous, *Radio Propagation Measurement and Channel Modelling*. John Wiley & Sons, Ltd, 2013.

[12] C. Matzler, "Microwave permittivity of dry sand," *IEEE Transactions on Geoscience and Remote Sensing*, 1998.

[13] C. Warren, A. Giannopoulos, and I. Giannakis, "gprMax: Open source software to simulate electromagnetic wave propagation for Ground Penetrating Radar," *Computer Physics Communications*, 2016.